

Interface between intramembranous and endochondral ossification in human fetuses

S. Hayashi¹, J.H. Kim², S.E. Hwang³, S. Shibata⁴, M. Fujimiya⁵, G. Murakami⁶, B.H. Cho⁷

¹Department of Anatomy, Tokyo Medical University, Tokyo, Japan

²Department of Anatomy, Chonbuk National University Medical School, Jeonju, Korea

³Department of Surgery, Daejeon Sun Hospital, Daejeon, Korea

⁴Maxillofacial Anatomy, Department of Maxillofacial Biology, Tokyo Medical and Dental University Graduate School, Tokyo, Japan

⁵Department of Anatomy, Sapporo Medical University School of Medicine, Sapporo, Japan

⁶Division of Internal Medicine, Iwamizawa Kojin-kai Hospital, Iwamizawa, Japan

⁷Department of Surgery and Research Institute of Clinical Medicine, Chonbuk National University Hospital, Jeonju, Korea

[Received 16 May 2013; Accepted 29 June 2013]

In the head and neck of human mid-term fetuses, the interface between areas of endochondral ossification and adjacent membranous (intramembranous) ossification is extensive. Using 8 foetal heads at 15–16 weeks, we have demonstrated differences in the matrices and composite cells between these 2 ossification processes, especially in the occipital squama and pterygoid process. Aggrecan-positive cartilage was shown to be invaded by a primitive bony matrix that was negative for aggrecan. At the interface, the periosteum was continuous with the perichondrium without any clear demarcation, but tenascin-c expression was restricted to the periosteum. In contrast, the interface between the epiphysis and shaft of the femur showed no clear localisation of tenascin-c. Versican expression tended to be restricted to the perichondrium. In the pterygoid process, the density of CD34-positive vessels was much higher in endochondral than in membranous ossification. The membranous part of the occipital was considered most likely to contribute to growth of the skull to accommodate the increased volume of the brain, while the membranous part of the pterygoid process seemed to be suitable for extreme flattening under pressure from the pterygoid muscles. (Folia Morphol 2014; 73, 2: 199–205)

Key words: endochondral ossification, intramembranous ossification, aggrecan, versican, tenascin-c, pterygoid process, occiput, human foetus

INTRODUCTION

The processes of endochondral and membranous (intramembranous) ossification control skeletogenesis. In contrast to endochondral ossification, in which cartilage is replaced by bone, membranous or mesenchymal ossification involves direct mineralisation of highly vascular connective tissue, in which osteoprogenitor cells proliferate densely around the capillary network [3]. In our recent study of elastic

fibres in the head and neck of mid-term fetuses [7, 9], elastica-Masson staining clearly demonstrated the morphology of the interface between membranous (Fig. 1 — green colour) and endochondral (Fig. 1 — blue colour) ossification. It was noteworthy that the 2 coloured matrices were not clearly demarcated, but showed mutual intercalation. This prompted us to conduct the present study. Previous descriptions of the interface morphology have usually focused on an

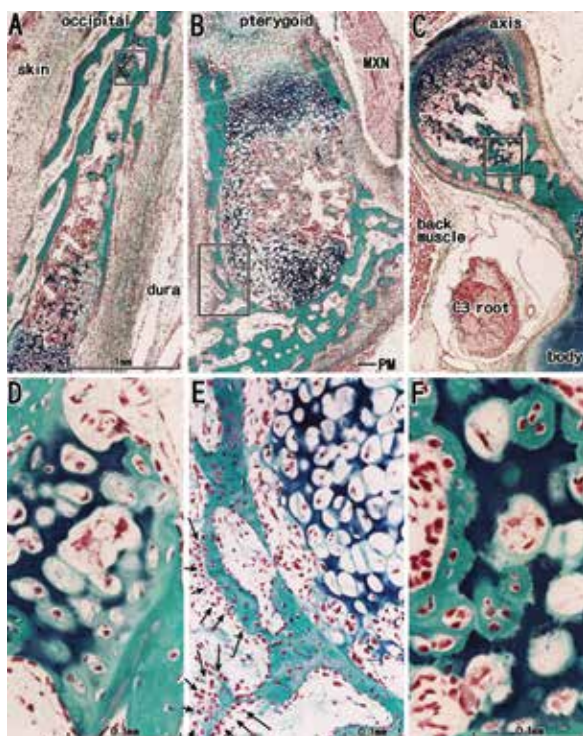


Figure 1. Interface between areas of membranous and endochondral ossification in the foetal head and neck. Sagittal sections of the head. All panels show elastica-Masson staining; **A, D.** Occiput; **B, E.** Pterygoid process; **C, F.** The spinous process of the axis or the second cervical vertebra. In the occiput and pterygoid, the upper side of the panel corresponds to the superior side of the head. Panels **D–F** display higher-magnification views of the square in panels **A–C**, respectively. Membranous ossification is coloured bright green, while endochondral ossification is coloured deep blue. The area of membranous ossification in the pterygoid is surrounded by the pterygoideus medialis muscle (PM). Arrows in panel **E** indicate a lining of osteoprogenitor cells. C3 root — 3rd cervical nerve root; MXN — maxillary nerve in the foramen rotundum.

area between the epiphysis cartilage and the periosteal collar of long bones in the extremities of children (i.e. Williams [23]). However, unlike the situation in the extremities, the interface has been shown to be long, large, or dispersed in the occipital (the squama; Fig. 1A), temporal (the squama and sites around the inner ear tubal structures), frontal, pterygoid process (Fig. 1B), mandibular and vertebral processes (Fig. 1C).

The major events of membranous ossification occur in the periosteum, whereas the area of endochondral ossification is enclosed by the perichondrium. However, the periosteum is continuous with the perichondrium, and shows no clear demarcation. In the developing chick tibiotarsal bone, Bandyopadhyay et al. [2] demonstrated perichondrium-specific as well as periosteum-specific transcriptional factors. Likewise, according to Michi-

kami et al. [13], Krüppel-like factor 4, which regulates osteocalcin, is expressed in the perichondrium of mouse long bones, but not in the periosteum. Nevertheless, despite such recent advances in molecular biology, there appears to be no information connecting a specific gene (or factor) with a matrix substance or cell component specific for each of the processes of membranous and endochondral ossification. Typically, type I collagen is absent in endochondral ossification, whereas hyaluronan (hyaluronic acid) is absent in membranous ossification [5]. The aim of the present study was to demonstrate differences in the matrices and composite cells between these 2 ossification processes in the human foetal head. For the our study purpose, we have chosen the occipital squama and the pterygoid process, because at the interface of these areas many sections can be easily obtained. Although the interface between the mandibular base (membranous ossification) and the anterior-most part of Meckel's cartilage (endochondral ossification) is also of interest in relation to formation of the torus mandibularis [17, 19], we have not focused on it here because, unlike other areas, Meckel's cartilage maintains a cartilaginous morphology for a long period.

MATERIALS AND METHODS

The study was performed in accordance with the provisions of the Declaration of Helsinki 1995 (as revised in Edinburgh 2000). We have observed the paraffin-embedded histology of 8 mid-term fetuses with an estimated gestational age of 15–16 weeks (crown-rump length 102–120 mm). With the agreement of the families concerned, these specimens had been donated to the Department of Anatomy, Chonbuk National University, Korea, and their use for research had been approved by the university ethics committee. Without breaking any rules of the universities or hospital, authors other than those affiliated to Chonbuk University were not required to inform the corresponding committees in Japan of this research project. All of the fetuses had been obtained by induced abortion. After the abortion, each of the mothers was personally informed by an obstetrician about the possibility of donating the foetus for research: no attempt was made to encourage donation. Because of randomisation of the specimen numbering, it was not possible to trace any of the families concerned.

The donated fetuses had been fixed in 10% w/w neutral formalin solution for more than 1 month. After the division into the head and neck, thorax, abdomen, pelvis and the 4 extremities, all parts were decalcified by incubation at 4°C in a 0.5-mol/L EDTA

solution (pH 7.5; decalcifying solution B; Wako, Tokyo) for 1–3 days, depending on the size of the material. Depending on their size, the head and neck specimens were cut into sagittal or horizontal sections 5 μm thick at the intervals of 20–50 μm . Each section included not only the brain, but also the surrounding structure such as the eye and ear. Thus, the skull base cartilages were available as a positive control for immunohistochemical procedures (see below). In addition, we have prepared longitudinal sections of the lower thigh including the epiphysis and shaft of the femur for comparison with the head and neck.

The sections were subjected to: 1) elastica-Masson staining; 2) immunohistochemistry for matrix substances and cell components; and 3) staining for hyaluronan. In the latter case, a biotinylated hyaluronan-binding protein (2 $\mu\text{g}/\text{mL}$; Seikagaku Corp., Tokyo, Japan) was used after the immersion of the sections in chondroitinase ABC (10 $\mu\text{U}/\text{mL}$; Seikagaku Corp.) in 0.1 M Tris-acetate buffer (pH 8.0, 37°C) for 30 min [18]. The elastica-Masson staining, a variation of Masson-Goldner staining, was based on that used by Motohashi et al. [14], Okada et al. [16] and Hayashi et al. [6].

The primary antibodies against matrix substances were: 1) mouse monoclonal anti-aggrecan core protein (12/21/1C6) from Developmental Studies Hybridoma Bank (Iowa City, IA, USA; dilution 1:25); 2) mouse monoclonal anti-versican core protein (12C5) from Developmental Studies Hybridoma Bank (dilution 1:25); 3) rabbit polyclonal anti-rat tenascin-c (Chemicon, Temecula, CA, USA; dilution 1:100); and 4) rabbit polyclonal anti-rat type I collagen (LSL, Tokyo, Japan; dilution 1:400). These matrix antibodies had been used in our previous immunohistochemical studies [18, 21]. All sections were treated with testicular hyaluronidase (25 mg/mL; Sigma type I-S; Sigma Chemicals, St Louis, MO, USA) in phosphate-buffered saline for 30 min at 37°C before the addition of the primary antibodies. After incubation for 30 min in a Histofine SAB kit (Nichirei, Tokyo, Japan) for the 3-amino-9-ethylcarbazole (AEC) reaction or in Histofine Simple Stain Max-PO (Nichirei, Tokyo, Japan) for the diaminobenzidine (DAB) reaction with horseradish peroxidase (HRP), the red biotin complex (AEC reaction) or dark brown colouration (DAB reaction) were obtained. Sections stained using DAB method were counterstained with haematoxylin.

The primary antibodies used for staining of cellular components were: 1) mouse monoclonal anti-human S100 protein (dilution 1:100; Dako Z0311; Dako, Glostrup, Denmark); 2) mouse monoclonal anti-human vi-

mentin (1:10; Dako M7020, Glostrup, Denmark); 3) rabbit monoclonal anti-human CD68 (1:100, Dako H7122, Glostrup, Denmark); 4) mouse monoclonal anti-human CD34 class II (dilution 1:100; Dako M7165, Glostrup, Denmark); 5) mouse monoclonal anti-human proliferating cell nuclear antigen (PCNA) (dilution 1:1000; Abcam ab29, Cambridge, UK). Pretreatment autoclaving was not conducted because of the loose nature of the foetal tissues. The secondary antibody (Dako Chem Mate Envison Kit, Dako, Glostrup, Denmark) was labelled with horseradish peroxidase (HRP), and antigen-antibody reactions were detected via the HRP-catalysed reaction with diaminobenzidine. Counterstaining with haematoxylin was performed on the same samples. S100 protein and vimentin are ossification markers, while CD68 is an osteoclast marker [7]. CD34 is a vascular marker [1, 8, 20] although, in adults, it is a major marker for mesenchymal and vascular progenitor cells [12, 22].

RESULTS

Observations of the occipital and pterygoid processes

The occipital behind the brain cavity was composed of a small and cuboidal condyle and a wide and flat squama. The condyle formed a convex-like articular surface with the atlas. In front of the brain cavity, the condyle continued to the basilar part of the occipital and the latter was connected with the cartilaginous otic capsule. In the wide and flat squama, the central part to which the back muscles were attached, was cartilaginous and relatively thick: endochondral ossification occurred in a small area below the muscle attachment, as well as in a wide area above it. The upper area of endochondral ossification was continuous and intermingled with the area of membranous ossification extending to the top of the head (Figs. 1A; 2). Because of scattered islands of transformed cartilage cells, the primitive bony matrix of the membranous ossification appeared to absorb the cartilages that should be connected mutually before. The perichondrium, as well as the periosteum, were much thicker on the dural side than on the skin side: neither contained elastic fibres. The labyrinth of the primitive bony matrix was rather simple, being straight and linear or plate-like, and enclosing vessels and transforming mesenchyme. The enclosed mesenchymal cells were polygonal or cuboidal, and formed an incomplete layer of polarised osteoblasts. The plate-like bony matrix appeared to invade into

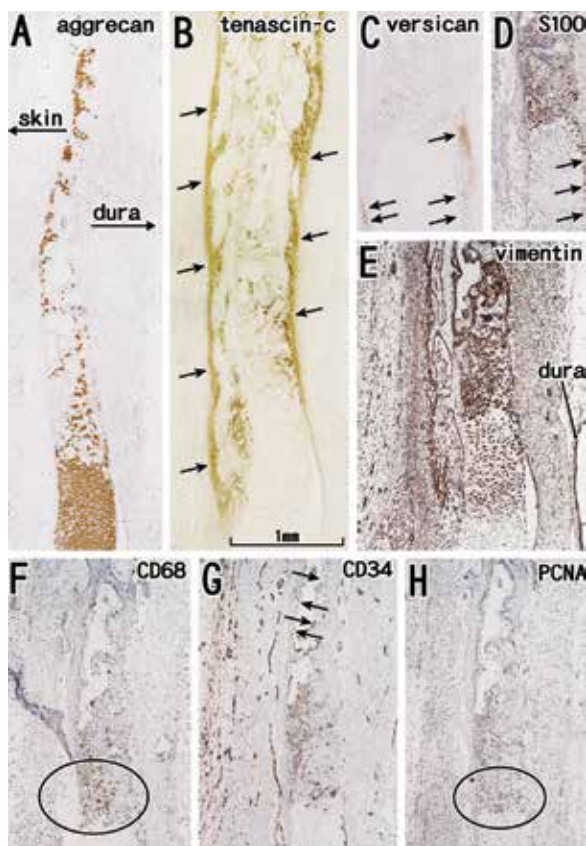


Figure 2. Immunohistochemistry of occipital osteogenesis. Sagittal sections of the head. The same specimen as that shown in Figure 1; **A.** Aggrecan; **B.** Tenascin-c; **C.** Versican; **D.** S100 protein; **E.** Vimentin; **F.** CD68; **G.** CD34; **H.** PCNA. Aggrecan expression overlaps with and occupies areas larger than the area coloured blue by elastica-Masson staining (see also Fig. 1A). Tenascin-c expresses in the periosteum (arrows in panel B). Reactivities for versican and S100 protein are evident in the perichondrium (arrows in panels C and D). Vimentin is expressed in transformed chondrocytes as well as osteoprogenitor cells. CD68-positive macrophages, as well as proliferating cells, are seen to have accumulated in the area of endochondral ossification (circle in panels F and H). A candidate bone marrow space (arrows in panel G), as well as many primitive vessels, are positive for CD34.

the area of cartilage; thus spotty cartilage fragments were seen in the membranous labyrinth. In the area of endochondral ossification, the transformed cartilage did not form a clear zone, but protruded into the area of membranous ossification.

The pterygoid process was an independent mass of cartilage behind the eyeball with a mushroom-like shape, the apex of which faced in an antero-inferior direction towards the maxilla and mandible. The surface of the outer dome was covered by thick mesenchymal tissue, in which membranous ossification was evident. In the cartilaginous pterygoid process, endochondral ossification was seen along the superficial surface, and thus most of the surfaces were

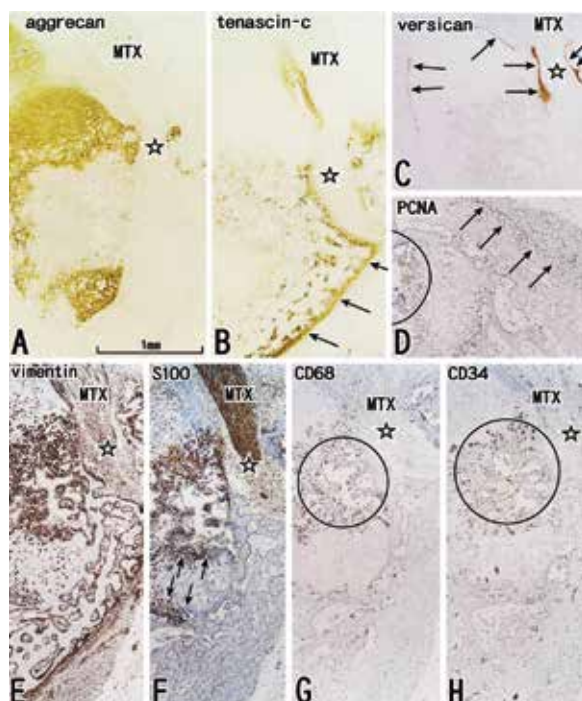


Figure 3. Immunohistochemistry of pterygoid osteogenesis. Sagittal sections of the head. The same specimen as that shown in Figures 1 and 2; **A.** Aggrecan; **B.** Tenascin-c; **C.** Versican; **D.** PCNA; **E.** Vimentin; **F.** S100 protein; **G.** CD68; **H.** CD34. Most panels other than panel D contain the maxillary nerve (MTX) in the foramen rotundum (clear star). Aggrecan expression overlaps with and occupies areas smaller than the area coloured blue by elastica-Masson staining (see also Fig. 1B). Tenascin-c is expressed in the periosteum (arrows in panel B). Reactivity for versican is evident in the perichondrium, especially along the foramen rotundum (arrows in panel C). Proliferating cells have accumulated in the periosteum, as well as in the area of endochondral ossification (arrows and a semi-circle in panel D). Vimentin is expressed in transformed chondrocytes as well as in osteoprogenitor cells (panel E). S100 protein reactivity is evident at the periphery of the area of endochondral ossification (arrows in panel F). CD68-positive macrophages, as well as CD34-positive vessels, are seen to have accumulated in the area of endochondral ossification (circle in panels G and H).

surrounded by membranous ossification. The transformed chondrocytes were adjacent, or close, to the labyrinth of the primitive bony matrix of membranous ossification. Conversely, the transformed cartilage did not form a clear zone. In contrast to the occipital squama, the cartilage area and the primitive bone matrix were relatively clearly demarcated. The maxillary nerve passed through the anterosuperior part of the pterygoid process, i.e. the foramen rotundum (Figs. 1B; 3). The membranous bone labyrinth was delicate and complex due to the presence of multiple trabeculae. Numerous osteoblasts were arranged in line along the trabeculae, and some of them were enclosed by a matrix of primitive lacunae.

In both the occipital and pterygoid, aggrecan-positive areas or cartilages overlapped with the areas stained blue with elastica-Masson (Figs. 2A; 3A). However, in the pterygoid process, the aggrecan-positive area appeared to be smaller than the blue coloured area. Tenascin-c was expressed in the periosteum, and this was clearly evident in the occipital squama (Fig. 2B). Bony surfaces along the foramen rotundum showed strong reactivity for tenascin-c (Fig. 3B). PCNA-positive proliferating cells were also densely distributed along the foramen (Fig. 3D). Reactivities for versican and S100 protein were evident in the perichondrium of the occipital squama (Fig. 2C, D) and in the periphery of the area of endochondral ossification in the pterygoid process (Fig. 3C, F). Vimentin was expressed in transformed chondrocytes, as well as in osteoprogenitor cells (Figs. 2E; 3E). CD68-positive macrophages, as well as proliferating cells, were found to have accumulated in the area of endochondral ossification (Figs. 2F, H; 3D, G). A candidate bone marrow space in the occipital was positive for CD34. The relatively clear zone of demarcation between the cartilage area and the primitive bone matrix in the pterygoid process carried few vimentin-positive cells and PCNA-positive cells; this low cell density along the demarcation was confirmed by elastica-Masson staining (Fig. 1E). In the pterygoid process, the density of CD34-positive vessels was much higher in the area of endochondral ossification than in the area of membranous ossification. CD34 and vimentin were positive in the cytoplasm, while S100 and CD68 appeared to be positive both in the cytoplasm and nucleus.

Observations of the femur

The epiphysis cartilage was attached to the periosteal collar in a limited area along the femoral surface. Thus, the cartilage did not intermingle with the area of membranous ossification. In the epiphysis, the transformed cartilage formed a clear zone that was positive for aggrecan and hyaluronan, but negative for type I collagen and versican (Fig. 4). The periosteal collar was not clearly identified because of weak expression of tenascin-c and the pale green colour resulting from elastica-Masson staining.

DISCUSSION

The epiphysis and periosteal collar of long bones form a well known interface between areas of endochondral and membranous ossification. Each zone, from the transformation of chondrocytes until cell death, can be clearly identified. However, the

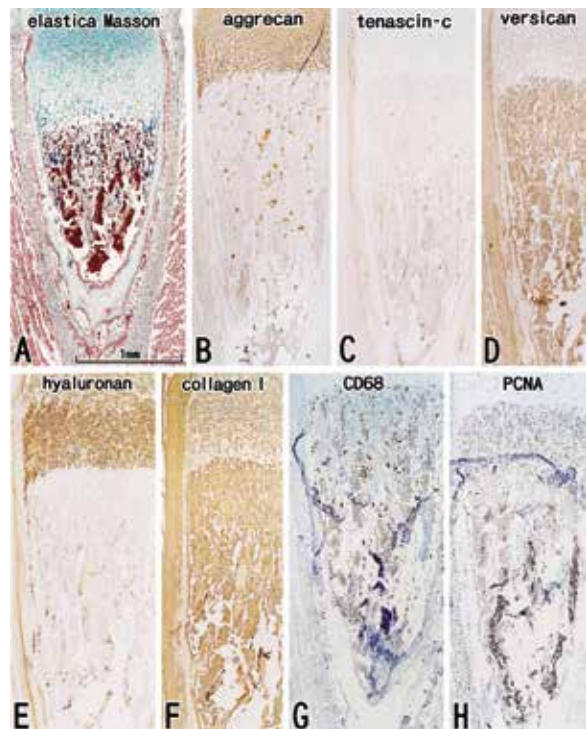


Figure 4. Immunohistochemistry of femoral osteogenesis. Longitudinal sections along the femoral shaft; **A.** Elastica-Masson staining; **B.** Aggrecan; **C.** Tenascin-c; **D.** Versican; **E.** Hyaluronan; **F.** Type I collagen; **G.** CD68; **H.** PCNA. Transformed cartilage is positive for aggrecan and hyaluronan, but negative for type I collagen and versican. The periosteal collar is not clearly identified because of weak expression of tenascin-c and the pale green colour resulting from elastica-Masson staining.

interface is restricted to within a point or a line around the bone surface. Moreover, the interface moves rapidly according to the growth of the long bone. In contrast, foetal head and neck cartilages are sometimes accompanied by a large area of membranous ossification. Thus, in mid-term foetuses, the occipital squama and pterygoid process would appear to be a better model for showing the difference in matrices and cell components at the interface. Tenascin-c appears to be the best example for this purpose: at the interface, the periosteum is continuous with the perichondrium without any clear demarcation, but tenascin-c expression is restricted to the periosteum. However, tenascin-c is also likely to be positive in the perichondrium, which provides attachment for muscles in the human limb girdle (unpublished data). Thus, it is not possible to state that tenascin-c is specific to the periosteum around an area of membranous ossification. Rather than such a dichotomy between periosteum and perichondrium, tenascin-c may be positively expressed in membranes covering

any foetal bone or cartilage that is undergoing an active remodelling process. The membranous bone in the occipital squama needs to undergo rapid changes in shape according to the increased volume of the brain, while the membranous bone in the pterygoid process becomes flattened by strong pressure from the pterygoid muscles.

The blue colour of the cartilage matrix produced by elastica-Masson staining mostly corresponded to areas of aggrecan expression. Because of scattered islands of transformed cartilage cells in the occipital squama, the primitive bony matrix of membranous ossification appeared to absorb the cartilages that should be connected mutually before. In contrast, the cartilage in the pterygoid appeared to maintain a round shape under a possible stressful condition, being surrounded by an area of membranous ossification. However, CD68-positive macrophages were greater in number along the ossification interface in the pterygoid process than in the occipital squama. In the pterygoid process, PCNA-positive cells were accumulated in line along the surface of periosteum. Thus, the outward growth of the membranous bone might interfere with the absorption of the cartilage part. In addition, S100 protein-positive chondrocytes were seen at the interface in the pterygoid process, as well as along the dural surface of the occipital squama. As Jin et al. [7] have suggested in the anterior longitudinal ligament of the vertebrae, these S100-positive cells may contribute to remodelling.

In spite of the relatively clear area of demarcation between endochondral and membranous ossification, a random and scattered arrangement of cells was evident in the pterygoid process. According to a well known review by Kronenberg [11], the perichondrium consists of an outer fibrous layer and an inner osteoprogenitor cell layer. However, in the pterygoid process, the cartilage appeared to lack any perichondrium facing the membranous bone. Membranous ossification is generally accompanied by highly vascular connective tissue. Nevertheless, in the pterygoid process, the density of CD34-positive vascular tissue was much higher in the area of endochondral ossification than in the area of membranous ossification. Therefore, cell components and matrices in the area of membranous ossification seemed to differ slightly between sites, at least between the occipital squama and the pterygoid process. One crucial and well characterised transcription factor involved in the process of differentiation of both chondrocytes

and osteoblasts is Runx2, which is expressed mainly in prehypertrophic and hypertrophic chondrocytes, as well as in perichondral cells and osteoblasts (reviewed by Komori [10]). Runx2 is also necessary for a tissue-specific genetic programme that regulates the production of vascular endothelial growth factor [4, 15]. However, because of the possible heterogeneity of membranous ossification in the foetal head, redundancy or modification of the Runx2 system may occur in the areas of membranous ossification.

Limitations of the study

The major limitation of this study was a fact that stages examined was limited in the mid-term. We needed to compare the present result with the late stage fetuses, but our larger materials did not express matrix substances, especially tenascin-c, possibly due to lag time after the death.

CONCLUSIONS

Consequently, in the interface between endochondral and membranous ossification processes in human fetuses, tenascin-c expression tended to be restricted to the periosteum, although site-dependent difference might be present.

ACKNOWLEDGEMENTS

This study was supported by a grant (0620220-1) from the National R & D Programme for Cancer Control, Ministry of Health and Welfare, Republic of Korea.

REFERENCES

1. Abe S, Suzuki M, Cho KH, Murakami G, Cho BH, Ide Y (2011) CD34-positive developing vessels and other structures in human fetuses: an immunohistochemical study. *Surg Radiol Anat*, 33: 919–927.
2. Bandyopadhyay A, Kubilus JK, Crochiere ML, Linsenmayer TF, Tabin CJ (2008) Identification of unique molecular subdomains in the perichondrium and periosteum and their role in regulating gene expression in the underlying chondrocytes. *Dev Biol*, 321: 162–174.
3. Colnot C, Lu C, Hu D, Helms JA (2004) Distinguishing the contributions of the perichondrium, cartilage, and vascular endothelium to skeletal development. *Dev Biol*, 269: 55–69.
4. Conen KL, Nishimori S, Provot S, Kronenberg HM (2009) The transcriptional cofactor Lbh regulates angiogenesis and endochondral bone formation during fetal bone development. *Dev Biol*, 333: 348–358.
5. Hall BK, Miyake T (1992) The membranous skeleton: the role of cell condensation in vertebrate skeletogenesis. *Anat Embryol*, 186: 107–124.
6. Hayashi T, Kumasaka T, Mitani K, Yao T, Suda K, Seyama K (2010) Loss of heterozygosity on tuberous sclerosis complex genes in multifocal micronodular pneumatoctyic hyperplasia. *Mod Pathol*, 23: 1251–1260.

7. Jin ZW, Song KJ, Lee NH, Nakamura T, Fujimiya M, Murakami G, Cho BH (2011) Contribution of the anterior longitudinal ligament to ossification and growth of the vertebral body: an immunohistochemical study using the human fetal lumbar vertebrae. *Surg Radiol Anat*, 33: 11–18.
8. Katori Y, Kiyokawa H, Kawase T, Murakami G, Cho BH (2011) CD34-positive primitive vessels and fascial structures in the ear, nose and throat of human fetuses: an immunohistochemical study. *Acta Otolaryngol*, 131: 1086–1090.
9. Kinoshita H, Umezawa T, Omine Y, Kasahara M, Rodríguez-Vázquez JF, Murakami G, Abe S (2013) Distribution of elastic fibers in the head and neck: a histological study using late-stage human fetuses. *Anat Cell Biol*, 16: 39–48.
10. Komori T (2010) Regulation of bone development and extracellular matrix protein genes by RUNX2. *Cell Tissue Res*, 339: 189–195.
11. Kronenberg HM (2003) Developmental regulation of the growth plate. *Nature*, 423: 332–336.
12. Lin CS, Xin ZC, Deng CH, Ning H, Lin G, Lue TF (2010) Defining adipose tissue-derived stem cells in tissue and in culture. *Histol Histopathol*, 25: 807–815.
13. Michikami I, Fukushi T, Tanaka M, Egusa H, Maeda Y, Ooshima T, Wakisaka S, Abe M (2012) Krüppel-like factor 4 regulates membranous and endochondral ossification. *Exp Cell Res*, 318: 311–325.
14. Motohashi O, Suzuki M, Shida N, Umezawa T, Ohtoh Y, Sakurai Y, Yoshimoto T (1995) Subarachnoid haemorrhage-induced proliferation of leptomeningeal cells and deposition of extracellular matrices in the arachnoid granulations and subarachnoid space. *Acta Neurochir*, 136: 88–91.
15. Nishimori S, Provot S, Kronenberg HM (2009) The transcriptional cofactor Lbh regulates angiogenesis and endochondral bone formation during fetal bone development. *Dev Biol*, 333: 348–358.
16. Okada R, Arima K, Kawai M (2002) Arterial changes in cerebral autosomal dominant arteriopathy with subcortical infarcts and leukoencephalopathy (CADASIL) in relation to pathogenesis of diffuse myelin loss of cerebral white matter. *Stroke*, 33: 2565–2569.
17. Rodríguez-Vázquez JF, Mérida-Velasco JR, Mérida-Velasco JA, Sánchez-Montesinos I, Espín-Ferra J, Jiménez-Collado J (1997) Development of Meckel's cartilage in the symphyseal region in man. *Anat Rec*, 249: 249–254.
18. Shibata S, Fukada K, Imai H, Abe T, Yamashita Y (2003) In situ hybridization and immunohistochemistry of versican, aggrecan, and link protein and histochemistry of hyaluronan in the developing mouse limb bud cartilage. *J Anat*, 203: 425–432.
19. Verdugo-Lopez S, Rodríguez-Vázquez, Garrido JM, Peinado-Real MA (2012) Torus mandibularis in the childhood and in the initial stages of adolescence. *Craniofacial Bone Res*, 1: 78–84.
20. Xu H, Edwards J, Banerji S, Prevo R, Jackson DG, Athanasou NA (2003) Distribution of lymphatic vessels in normal and arthritic human synovial tissues. *Ann Rheum Dis*, 62: 1227–1229.
21. Yokohama-Tamaki T, Maeda T, Tanaka TS, Shibata S (2011) Functional analysis of CTRP3/cartducin in Meckel's cartilage and developing condylar cartilage in the fetal mouse mandible. *J Anat*, 218: 517–533.
22. Young HE, Steele TA, Bray RA, Hudson J, Floyd JA, Hawkins K, Thomas K, Austin T, Edwards C, Cuzzourt J, Duenzi M, Lucas PA, Black AC Jr (2001) Human reserve pluripotent mesenchymal stem cells are present in the connective tissues of skeletal muscle and dermis derived from fetal, adult, and geriatric donors. *Anat Rec*, 264: 51–62.
23. Williams PL (1995) *Gray's anatomy*. 38th Ed. Churchill Livingstone, Edinburgh, pp. 471–480.